Sensitivity studies of circulation and ocean-shelf exchange off northern Norway

Helene Moseidjord, Harald Svendsen & Dag Slagstad

SARSIA

Moseidjord H, Svendsen H, Slagstad D. 1999. Sensitivity studies of circulation and ocean-shelf exchange off northern Norway. *Sarsia* 84:191-198.

Knowledge about the general circulation on the shelf off northern Norway on a sufficiently small scale to include the influence of the shelf topography has been achieved before, through field investigations. However, little is known about what controls the flow in this area on the small scale. The objective of this study was to find what possibly controls the flow, with special emphasis on shelf circulation and ocean-shelf exchange. Due to lack of sufficiently appropriate (small-scale, long-term) field data, an approach using a numerical model was adopted. Through model sensitivity experiments it was possible to study the effect of shelf topography and upwelling-favourable wind separately. Successful simulation of the general shelf circulation and vortex formations in agreement with field observations indicates that the model employed was performing realistically. There appears to be a strong correlation between the variation in the onshore flux in the Malangendypet trench and that in the along-shore wind component. The shelf topography seems to induce a complex wind-driven up-welling, with cross shelf trenches guiding the onshore flow. The shelf topography in combination with strong topographic steering appear to induce upwelling in areas where topographically steered currents leaving the shelf converge with the slope current.

Helene Moseidjord & Harald Svendsen, University of Bergen, Department of Geophysics, Allégt. 70, N-5007 Bergen, Norway. – Dag Slagstad, SINTEF Civil and Environmental Engineering, Coastal and Ocean Engineering, N-7465 Trondheim, Norway.*
**Present address: Statoil, PO Box 7200, N-5020 Bergen, Norway.*
E-mail: helemos@statoil.com – harald.svendsen@gfi.uib.no – dag.slagstad@civil.sintef.no

Keywords: Shelf; circulation; topographic steering; upwelling.

INTRODUCTION

The shelf off northern Norway is narrow compared to further south. The topography is dominated by cross-shelf trenches situated between rather flat banks. A steep continental slope separates the shelf from the deep Norwegian Sea.

The large scale flow and distribution of water masses along the Norwegian coast is well-known. The Norwegian coastal current advects relatively fresh water northward, whereas the North Atlantic Current, situated further offshore, advects more salty water of Atlantic origin northward, mainly along the continental slope. The interaction between the two is complex and a field of active research.

Knowledge about the general circulation on the shelf off northern Norway on a sufficiently small scale to include the influence of the shelf topography has been achieved before, through field investigations (Sundby 1984). The shelf topography was found to strongly influence the distribution of water masses and current pattern. Coastal water was found to perform anticyclonic rotation over the banks whereas Atlantic water intruding into the trenches was found to rotate cyclonically. However little is known about what controls the flow in this area on the small scale. E.g. what controls the flow into the trenches and what is the effect of upwelling-favourable wind in this connection?

The objective of this study was to find what possibly controls the flow, with special emphasis on shelf circulation and ocean-shelf exchange. Due to lack of sufficiently appropriate (small-scale, long-term) field data, an approach using a numerical model was adopted. Through model sensitivity experiments it was possible to study the effect of shelf topography and upwelling-favourable wind separately.

This project has character of a pilot study and is meant to form a basis for future investigations where field investigations should play an important role, especially for model validation purposes.

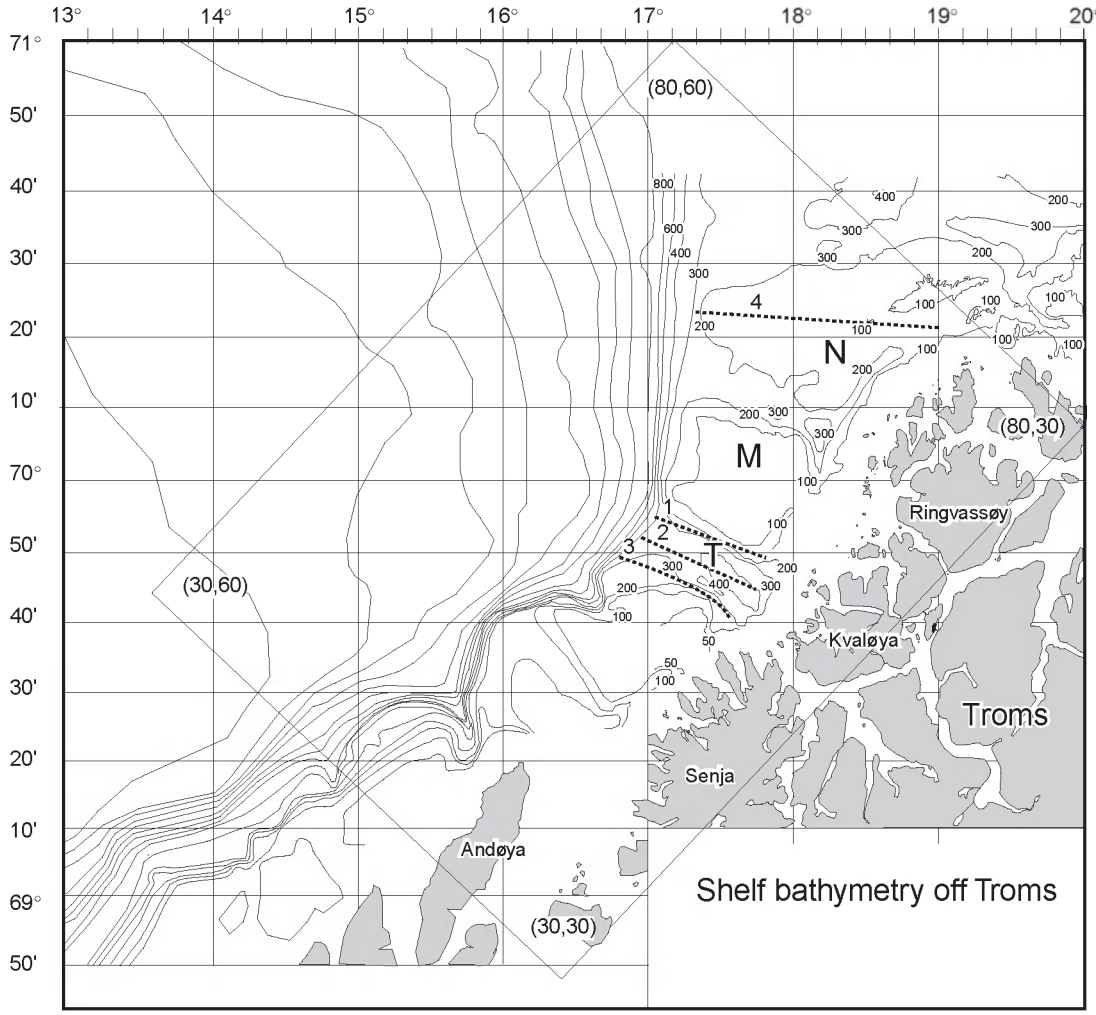

Fig. 1. Shelf bathymetry off northern Norway. N, M and T are the Nordvestbanken bank, the Malangsgrunnen bank and the Malangendypet trench respectively. ADCP sections are indicated as stippled lines (1-4).

METHOD

Model description

The numerical model applied is a 3-D, baroclinic, finite-difference, level (z-coordinate) model, mathematically defined by Equations 1-5:

The momentum equation (the fluid is assumed to be incompressible):

$$\frac{\partial \vec{u}}{\partial t} + \vec{u}\cdot\nabla\vec{u} + w\frac{\partial \vec{u}}{\partial z} + f\vec{k}x\vec{u} = -\frac{1}{\rho_o}\nabla p + A_H\nabla^2\vec{u} + \frac{\partial}{\partial z}\left(\nu\frac{\partial \vec{u}}{\partial z}\right) \quad (1)$$

the continuity equation:

$$\nabla\cdot\vec{u} + \frac{\partial w}{\partial z} = 0 \quad (2)$$

the hydrostatic equation

$$\frac{\partial p}{\partial z} = -\rho g \quad (3)$$

the equation for salinity and temperature

$$\frac{\partial \varphi}{\partial t} + \vec{u} \cdot \nabla \varphi + w \frac{\partial \varphi}{\partial z} = K_H \nabla^2 \varphi + \frac{\partial}{\partial z}\left(\nu \frac{\partial \varphi}{\partial z} \right) + \delta_\varphi \quad (4)$$

and the equation of state (UNESCO 1981)

$$\rho = \rho(S, T) \quad (5)$$

where

x, y, z	Cartesian coordinates
$\vec{i}, \vec{j}, \vec{k}$	unit vectors
t	time
$\vec{u}$	horizontal velocity vector
w	vertical velocity component
f	Coriolis parameter
g	acceleration due to gravity
p	pressure
ρ	density
ρ_0	= 1027.55 kgm^{-3}, reference density
A_H	= 10 m^{2}s^{-1} horizontal eddy viscosity
K_H	= 5 m^{2}s^{-1} horizontal eddy diffusivity
ν	vertical eddy viscosity and diffusivity
φ	salinity, S or temperature, T
δ_S	$\equiv 0$
δ_T	heat exchange between the sea surface and the atmosphere

$$\nabla = \vec{i}\frac{\partial}{\partial x} + \vec{j}\frac{\partial}{\partial y}$$

$$\nabla^2 = \vec{i}\frac{\partial^2}{\partial x^2} + \vec{j}\frac{\partial^2}{\partial y^2}$$

ν is a function of the Richardson number and the wind speed (for details see Slagstad & Stokke 1994).

A nesting procedure is applied to provide lateral boundary conditions. This procedure requires the model to be run for the same period of time also for a larger area (on a coarser grid), enclosing the area of study. A flow relaxation scheme (FRS) (Martinsen & Engedahl 1987) is used to perform a one way nesting from the coarse-grid, large-area model to the open boundaries of the fine-grid model. The FRS makes sure that there is a smooth transition from the open boundaries to the inner domain of the fine-grid model.

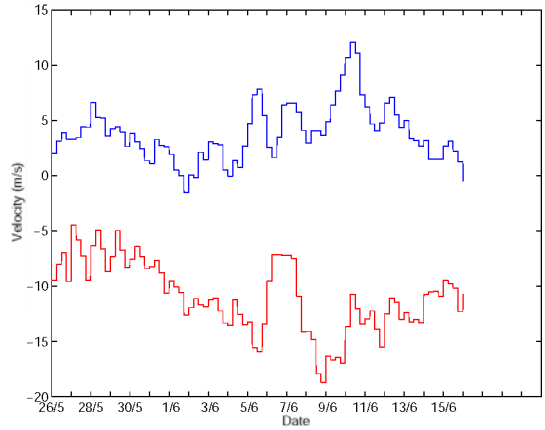

Fig. 2. Along-shore (red) and cross-shore (blue) wind components from gridpoint (55,45).

Information about the model setup for the two domains is given below. The data in brackets are for the coarse-grid model (the vertical resolution is the same for both domains).

Horizontal resolution	4 km (20 km)
Vertical resolution (from surface)	10 m, 6 × 5 m, 10 m, 6 × 25 m, 2 × 50 m, 100 m, 200 m, 400 m, 100 m, 200 m, 400 m, 1000 m
Number of horizontal gridpoints	125 × 100 (150 × 120)
External (barotropic) timestep	15 s (75 s)
Internal (baroclinic) timestep	6 min (30 min)

Further details about the model can be found in Slagstad (1987) (first version of the model), Slagstad & al. (1990), Støle-Hansen & al. (1989) and Slagstad & Stokke (1994).

Sensitivity experiments

The large-area model was for all experiments initiated from Levitus (1982) climatological data, and forced by predescribed in- and outflow across the open boundaries and heat exchange between the sea surface and atmosphere. The inflow along the Norwegian coast was given by McClimans (1993) and the data for calculation of heat exchange between the sea surface and atmosphere was from Norwegian Meteorological stations. For some of the experiments (specified later) atmospheric pressure and wind forcing (from the Norwegian Meteorological Institute's hindcast database) was applied. In Fig. 2 the time-series for the applied wind in gridpoint (55,45) is given. All the gridpoint references throughout the paper are for the fine grid (see Figs 3 and 4).

The fine-grid model was initiated and forced on the lateral boundaries by data from the large-area model. For the inner domain of the fine-grid model the same forcing was used as for the large-area model. The applied

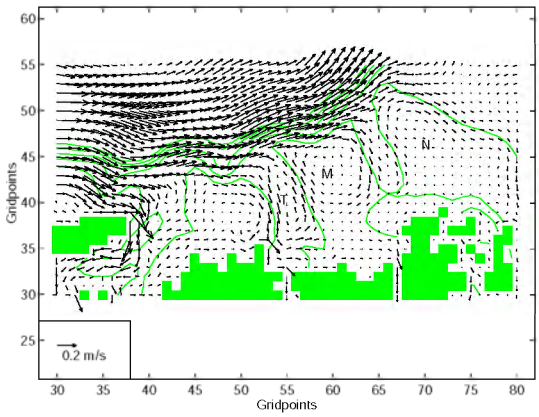

Fig. 3. Surface currents for experiment RE. Depth contours are plotted for each 200 m down to 1000 m.

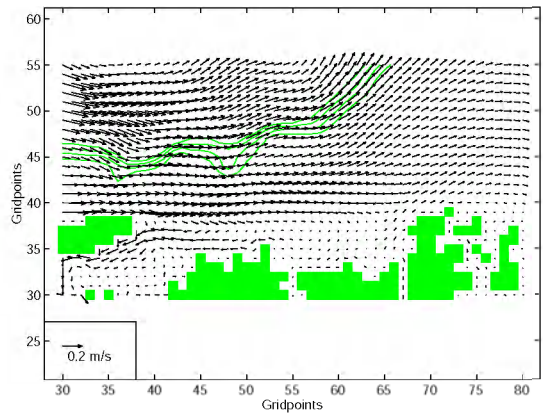

Fig. 4. Surface currents for experiment FE. Depth contours are plotted for each 200 m down to 1000 m.

forcing was intended to give a realistic flow field.

Two bathymetry matrices were applied for the fine-grid model; both were developed to represent the realistic bathymetry of the area, except in one of the matrices where the area representing the shelf was changed to represent a perfectly flat shelf. The depth of the flat shelf was chosen to be the average depth of the realistic shelf.

With the intention to study the effect of atmospheric forcing and topography on the shelf circulation and ocean-shelf exchange, sensitivity testes were performed with the fine-grid. In this pilot study the tests are limited to four scenarios i.e. four sensitivity experiments performed with the fine-grid model. The duration of each run was 21 days, from 26 May to 16 June 1987 (to coincide with the data used for forcing). A summary of each experiment is given below. Apart from the differences specified below, the experiments were identical.

RI	Realistic shelf - Including atmospheric forcing
RE	Realistic shelf - Excluding atmospheric forcing
FI	Flat shelf - Including atmospheric forcing
FE	Flat shelf - Excluding atmospheric forcing

Atmospheric forcing here includes atmospheric pressure and wind.

For each experiment, calculations of fluxes across a 24 km long section (from gridpoint (53,40) to (58,40)), situated about 20 km from the shelf break across the Malangsdjupet trench, were made. The calculations were split into onshore, offshore and net fluxes.

RESULTS

The flow on the shelf was largely determined by the bottom topography, with currents constrained by geostrophy to flow along depth contours (experiment RE). This can be seen from the surface currents in Fig. 3. Notice that, as also indicated in Fig. 3, there is a tendency of vortex formation above the shelf banks, especially above the Malangsgrunnen bank (M) where closed streamlines can be deduced from the velocity vectors. It is evident from comparison between Fig. 4, which represents the surface currents for the flat shelf experiment (FE), and Fig. 3 that the shelf topography has a strong influence on the flow, due to the fact that the current patterns are so different in the two cases.

The flux calculations for the Malangsdjupet trench showed large fluctuations at the start of the simulation (for experiment RE see Fig. 5) probably mainly due to the adjustment of the rather uniform initial velocity field to the complex shelf topography. About 10 days after simulation start only small fluctuations remained (O(0.01 Sv)) for the case with no wind (experiment RE). The calculations from then on showed nearly equal on- and offshore fluxes of about 0.2 Sv, which confirmed the

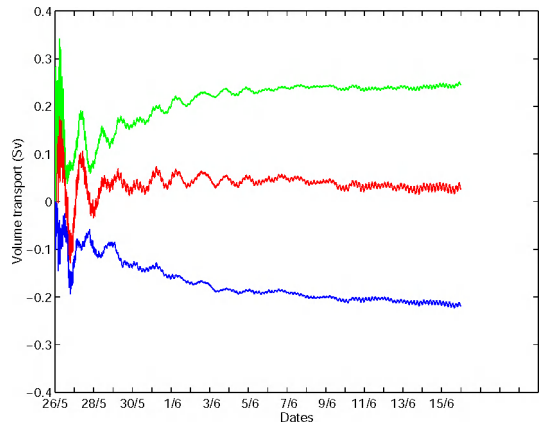

Fig. 5. Flux calculations for the Malangendypet trench for experiment RE: red = net flux, blue = onshore flux and green = offshore flux.

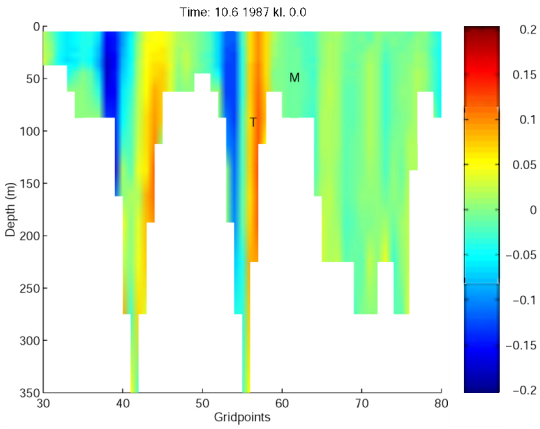

Fig. 6. Section from gridpoint (30,40) to (80,40) of cross-shelf flow for experiment RE. The velocities are given in ms^{-1} and positive values indicate offshore flow.

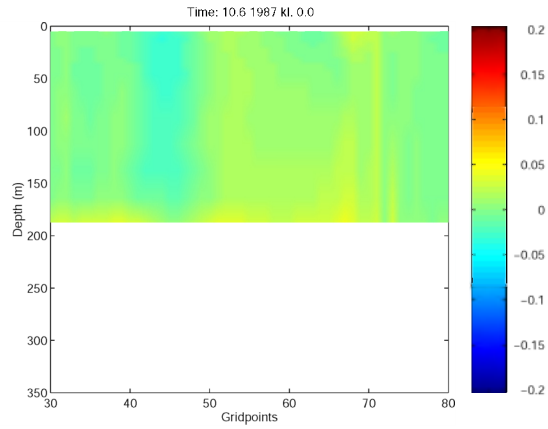

Fig. 7. Section from gridpoint (30,40) to (80,40) of cross-shelf flow for experiment FE. The velocities are given in ms^{-1} and positive values indicate offshore flow.

strong topographic steering on the shelf indicated by the surface currents in Fig. 3.

In Fig. 6 the section across the Malangsdjupet trench has been extended to show the cross shelf flow over a larger area. The deflection of the flow to circulate via the trenches is evident for the Malangsdjupet trench. Fig. 7 shows the same section for the flat shelf (experiment FE).

The applied wind totally altered the circulation on the shelf (experiment RI). The onshore flow in the Malangsdjupet trench (see Fig. 8) was generally larger than the offshore flow in this case. The flow has an increasing trend from the end of the "adjustment period" to about 6 June, i.e. during a period with increasing alongshore wind. The sudden drop in the onshore flow 6 June followed by a strong increase to a maximum flow 10 June coinciding with a similar variation pattern in the alongshore wind (sudden decrease during 6 June followed by an increase to a maximum 10 June). The maximum net onshore flux was about 0.15 Sv. In fact there appears to be a strong relation between the variation in the onshore flux in the Malangsdjupet trench and that in the along-shore wind component (compare Figs 2 and 8).

The strong topographic steering is also confirmed in the trajectories of the particles released off the coast of Lofoten (south of the model domain in Figs 3 and 4). The particles reaching the Malangsgrunnen bank and Nordvestbanken bank are trapped in vortices, Fig. 9, and may have a residence time varying from a few days to several weeks, Fig. 10.

The shelf topography induced a rather complex wind-driven upwelling (experiment RI); compared to the nearly

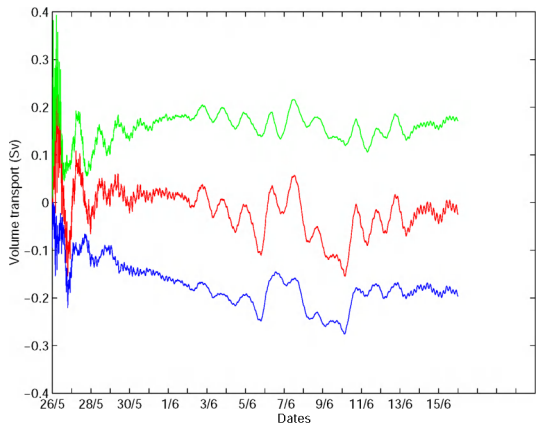

Fig. 8. Flux calculations for the Malangendypet trench for experiment RI; red = net flux, blue = onshore flux and green = offshore flux.

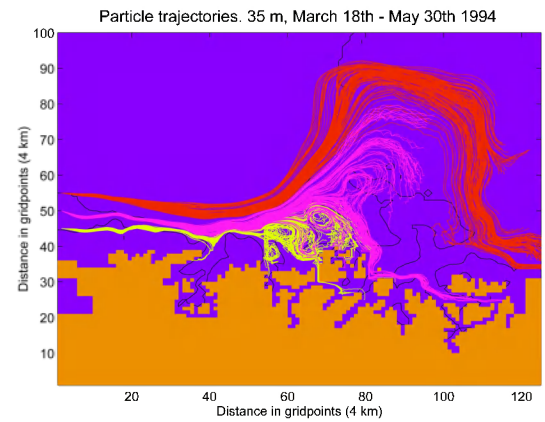

Fig. 9. Particle trajectories at 35 m depth simulated for the period March 18 - May 30 1994.

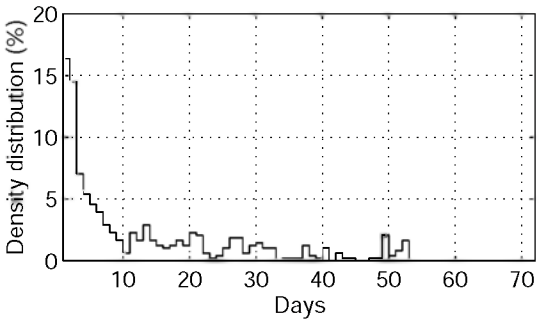

Fig. 10. Residence time for particles at the Nordvestbanken.

uniform (alongshore) response found for the flat shelf (experiment FI). For both experiments (RI and FI) water was transported offshore by the wind in the surface (Ekman layer), first generating and later maintaining a divergence by the coast. The onshore flow driven to feed the coastal divergence was rather uniform for the flat shelf (experiment FI, see Fig. 11) except in a narrow section normal to the coast around gridpoint 38. The yellow colour represents a weak offshore flow probably related to the large adjacent Andfjord basin, "the missing coastal wall" in this area, Fig. 3, creating an inflow with a compensating outflow in the basin.

The flow was guided by the cross shelf trenches in the more realistic case (experiment RI, see Fig. 12). The non-uniform onshore flow (experiment RI) caused a redistribution of water alongshore to take place, for an even distribution to the coastal divergence. During the period of strongest alongshore wind a jet developed by the coast, by the head of the Malangsdjupet trench, redistributing water southwards (experiment RI). The jet lasted for several days, Figs 13 and 14, and ceased when the alongshore wind decreased 10 June.

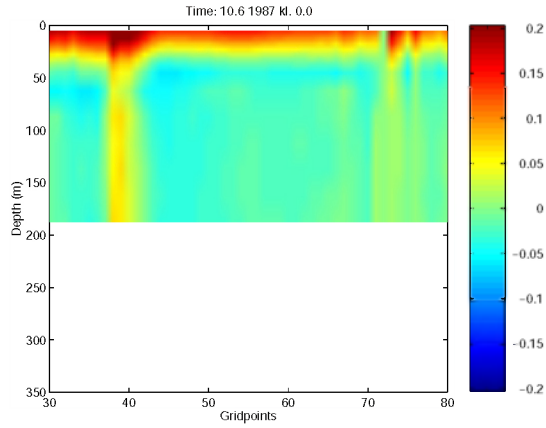

Fig. 11. Section from gridpoint (30,40) to (80,40) of cross-shelf flow for experiment FI. The velocities are given in ms^{-1} and positive values indicate offshore flow.

Topographically-induced upwelling was found in areas where topographically steered currents leaving the shelf converged with the slope current (experiments RI and RE), the result from experiment RE is given in Fig. 16. This upwelling ceased (experiment RI) during periods when strong alongshore wind disturbed the circulation on the shelf, reducing the driving force for the upwelling. As expected no topographically-induced upwelling was found for the flat shelf (experiments FI and FE).

DISCUSSION

An attempt to simulate the "true" flow field in an area as complex as off the coast of Troms and Finnmark is a severe, if not impossible, task. To succeed, all the major factors which determine the flow, i.e. what drives and

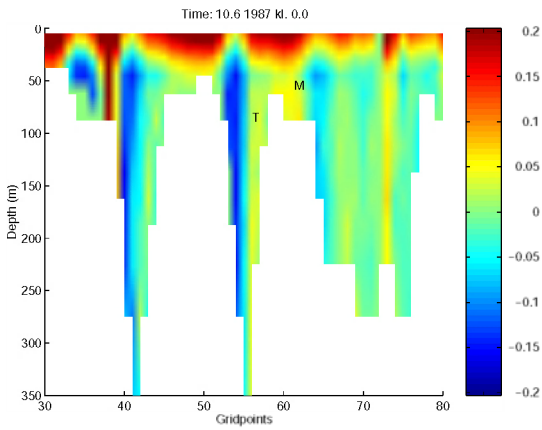

Fig. 12. Section from gridpoint (30,40) to (80,40) of cross-shelf flow for experiment RI. The velocities are given in ms^{-1} and positive values indicate offshore flow.

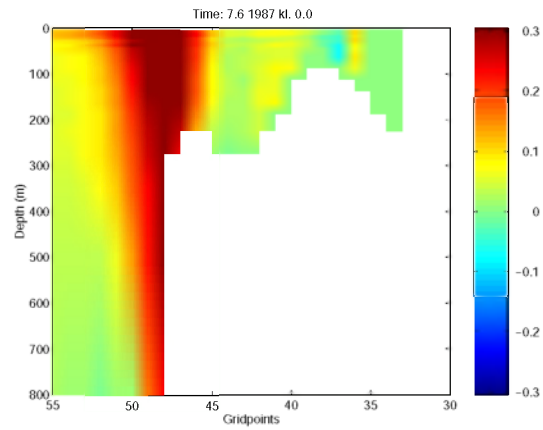

Fig. 13. Section from gridpoint (53,30) to (53,55) of along-shelf flow for experiment RI. The velocities are given in ms^{-1} and positive values indicate northward flow.

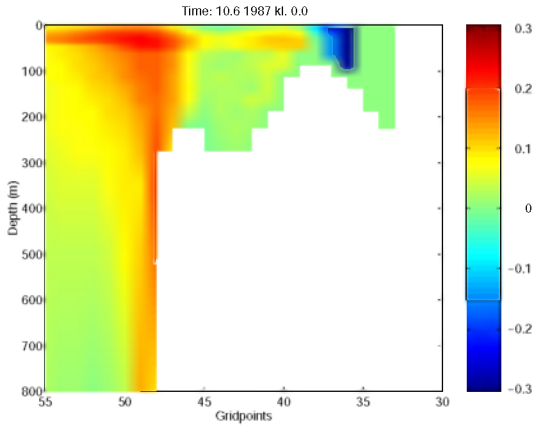

Fig. 14. Section from gridpoint (53,30) to (53,55) of along-shelf flow for experiment RI. The velocities are given in ms^{-1} and positive values indicate northward flow.

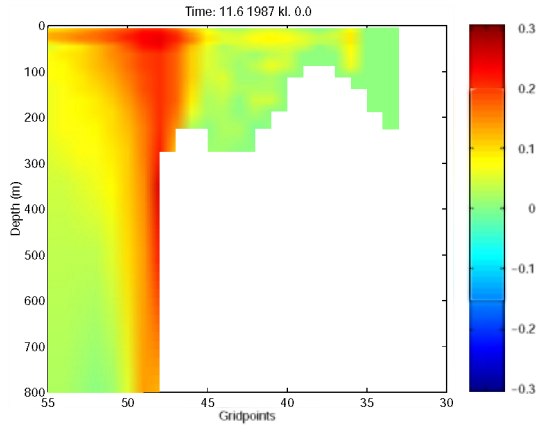

Fig. 15. Section from gridpoint (53,30) to (53,55) of along-shelf flow for experiment RI. The velocities are given in ms^{-1} and positive values indicate northward flow.

influences it, must be correctly represented. The major difficulty in this attempt was the presence of three open boundaries, with a steep continental slope passing through two of them. The nesting technique and the flow relaxation scheme were used to reduce this difficulty. The time dependent boundary conditions together with the other time dependent forcing, resulted in simulation results of high complexity.

The general shelf circulation simulated (experiment RE) agrees well with Sundby's (1984) tentative map of the circulation in the upper layer during almost homogeneous conditions (i.e. October-May) based on hydrographic data, trajectories of satellite-tracked buoys drogued in the surface mixed layer and the observed distribution of cod eggs. The vertical stability of the water column was relatively low in the simulations and of the same order of magnitude as during "homogeneous conditions" as described by Sundby (1984). Sundby (1984) observed the presence of vortices above the shelf banks from the horizontal temperature distribution (in 20 m depth) in one out of four surveys. This confirms that the tendency of vortex formation simulated (experiment RE) is a realistic temporal feature in the area.

The simulated circulation pattern is also in reasonable agreement with ADCP-sections taken along the Malangsdjupet trench (compare Fig. 3 and sections 1-3 in Fig. 17). An ADCP-section taken further north across the Nordvestbanken bank in March 1994 (section 4 in Fig. 17) indicates deflection of the currents around the bank and thus qualitatively confirms the model results. Vertical ADCP profiles (not shown) have an almost homogenous (barotropic) structure. A thorough examina-

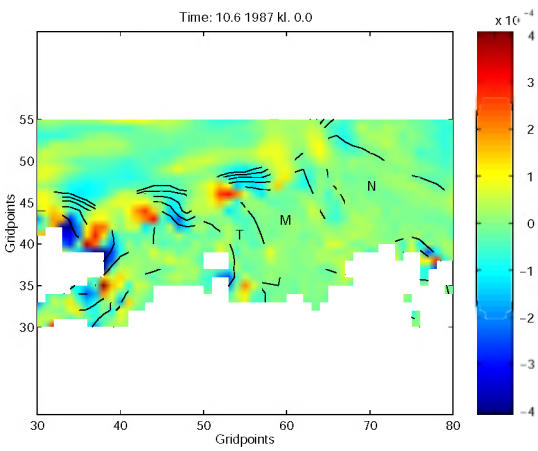

Fig. 16. Vertical velocity in 45 depth. The velocities are given in ms^{-1} and positive values indicate upwelling. Depth contours are plotted for each 200 m down to 1000 m.

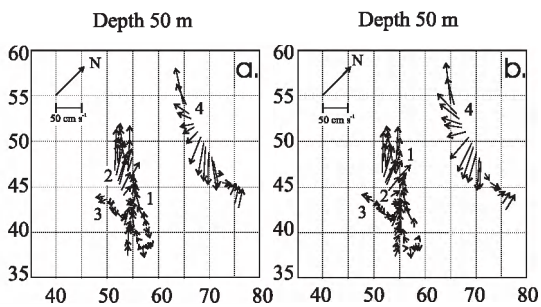

Fig. 17. a) Current velocity in 50 m depth taken from ADCP-sections along the Malangendypet trench (1, 2 and 3) and across the Nordvestbanken bank (4). The speed of the ship was 7 knots and the data are 15 min. averages. b) The same as a), but with the tide (modelled) subtracted. The vectors are plotted relative to the model grid. For the details about the ADCP-data and modelled tide see Nordby & al. 1999.

tion of the available ADCP-data has not been performed at this stage, so it is uncertain whether these strong currents are persistent on the bank or not.

An implication of the strong topographic steering in combination with the complex shelf topography and especially the presence of vortex formations, is a relatively long residence time for the water masses in the area. The residence time is believed to be of great importance for the marine environment in the area. During periods when the flow is partly decoupled from the topography by e.g. wind (friction) the residence time is believed to reduce.

Another implication of the strong topographic steering in combination with the complex shelf topography, is increased mixing (exchange) between ocean and shelf waters. The argument for this is that the frontal-line between the two water masses is elongated because of the "wavy" depth contours.

The wind-driven upwelling response simulated for the realistic shelf topography (experiment RI) is related to evidence found by Shaffer (1976) of cross shelf "canyons" guiding upwelling off north-west Africa. Also there the upwelling was found to be concentrated at the head of the "canyons" and a redistribution along-shore (by a coastal yet) was observed, as simulated here (experiment RI).

The fact that a similar wind-driven upwelling response has been observed in a shelf area with comparable bottom topography, increases the reliability of this simulation result. Sundby (1984) found that the intrusion of "Atlantic" water into the Malangsdjupet trench varies, but the reason was not understood. This work indicates that the variation is due to the changes in the alongshore wind-component. Other factors like stratification and current speed are also believed to be of importance, but these have not been investigated here.

No observational evidence for the topographically-induced upwelling has been found.

The main conclusions from the model results are:

- Successful simulation of the general shelf circulation and vortex formations in agreement with field observations, indicate that the model employed was performing realistically.
- There is an indication of a close relation between the strength of the along-shore wind and the variation of the onshore flux in the Malangsdjupet trench since the variations in the net onshore flux coincide with the variations in the along-shore wind.
- The shelf topography seems to induce a complex wind-driven upwelling, with cross shelf trenches guiding the resulting onshore flow. The shelf topography in combination with strong topographic steering appear to induce upwelling in areas where topographically steered currents leaving the shelf converge with the slope current.

Only future field investigations can detect the importance of these results.

ACKNOWLEDGEMENTS

This study was financially supported by the Research Council of Norway (project no. 101323/410 and 108085/122) and the European Commission (MAS2-CT93-0069 OMEX I and MAS3-CT96-0056 OMEX II).

REFERENCES

Levitus S. 1982. *Climatological Atlas of the World Ocean.* NOAA Prof Paper No. 13. 173 p.

Martinsen EA, Engedahl H. 1987. Implementation and testing of a lateral boundary scheme as an open boundary condition in a barotropic ocean model. *Coastal Engineering* 11:603-627.

McClimans TA. 1993. An algorithm for computing monthly averaged inflow of Atlantic water to the Norwegian Sea. *SINTEF NHL report* STF60 A93009.

Nordby E, Tande KS, Svendsen H, Slagstad D. 1999. Oceanography and fluorescence at the shelf break off the North Norwegian coast (69°20'N-70°30'N) during the main productive period in 1994. *Sarsia* 84:175-189.

Shaffer G. 1976. A mesoscale study of coastal upwelling variability off N.W. Africa. *Meteor Forschungsergebnisse* A17:21-72.

Slagstad D. 1987. A 4-Dimensional model of the Barents Sea. *SINTEF report* STF48 F87013.

Slagstad D, Støle-Hansen K, Loeng H. 1990. Density driven currents in the Barents Sea calculated by a numerical model. Modeling. *Identification and Control* 11(4):181-190.

Slagstad D, Stokke S. 1994. Simulation of current field, hydrography, ice cover and primary production in the northern Barents Sea. *Fisken og Havet* No. 9, 1994. 47 p.

Støle-Hansen K, Slagstad D, Utnes T. 1989. Baroclinic model test case information. *SINTEF report* STF48 F89002.

Sundby S. 1984. Influence of bottom topography on the circulation at the continental shelf off northern Norway. *Fiskeridirektoratets Skrifter Serie Havundersøkelser* 17:501-519.

UNESCO 1981. *Tenth Report of the Joint Panel on Oceanographic Tables and Standards.* UNESCO Technical Papers in Marine Science No. 36. p 24.

Accepted 17 April 1998 – Printed 15 November 1999
Editorial responsibility: Ulf Båmstedt